

Neutrino mass hierarchy determination and other physics potential of medium-baseline reactor neutrino oscillation experiments *

A.B. Balantekin¹³, H. Band^{14,13}, R. Betts⁷, J.J. Cherwinka¹³, J.A. Detwiler¹¹, S. Dye⁵, K.M. Heeger^{14,13}, R. Johnson³, S.H. Kettell¹, K. Lau⁶, J.G. Learned⁴, C.J. Lin², J.J. Ling¹, B. Littlejohn³, D.W. Liu⁶, K.B. Luk², J. Maricic⁴, K. McDonald⁹, R.D. McKeown¹², J. Napolitano¹⁰, J.C. Peng⁸, X. Qian¹, N. Tolich¹¹, W. Wang¹², C. White⁷, M. Yeh¹, C. Zhang¹, and T. Zhao¹¹

¹*Brookhaven National Laboratory, Upton, NY, USA*

²*University of California and Lawrence Berkeley National Laboratory, Berkeley, CA, USA*

³*University of Cincinnati, Cincinnati, OH, USA*

⁴*University of Hawaii, Honolulu, HA, USA*

⁵*Hawaii Pacific University, Kaneohe, HA, USA*

⁶*University of Houston, Houston, TX, USA*

⁷*Illinois Institute of Technology, Chicago, IL, USA*

⁸*University of Illinois at Urbana-Champaign, Urbana, IL, USA*

⁹*Princeton University, Princeton, NJ, USA*

¹⁰*Rensselaer Polytechnic Institute, Troy, NY, USA*

¹¹*University of Washington, Seattle, WA, USA*

¹²*College of William and Mary, Williamsburg, VA, USA*

¹³*University of Wisconsin, Madison, WI, USA*

¹⁴*Yale University, New Haven, CT, USA*

Abstract

Medium-baseline reactor neutrino oscillation (MBRO) experiments have been proposed to determine the neutrino mass hierarchy (MH) and to make precise measurements of the neutrino oscillation parameters. With sufficient statistics, better than $\sim 3\%/\sqrt{E(\text{MeV})}$ energy resolution and well understood energy non-linearity, MH can be determined by analyzing oscillation signals driven by the atmospheric mass-squared difference in the survival spectrum of reactor antineutrinos. With such high performance MBRO detectors, oscillation parameters, such as $\sin^2 2\theta_{12}$, Δm_{21}^2 , and Δm_{32}^2 , can be measured to sub-percent level, which enables a future direct unitarity test of the PMNS matrix to $\sim 1\%$ level and helps the forthcoming neutrinoless double beta decay experiments to constrain the allowed $\langle m_{\beta\beta} \rangle$ values. Combined with results from the next generation long-baseline beam neutrino and atmospheric neutrino oscillation experiments, the MH determination sensitivity can reach higher levels. In addition to the neutrino oscillation physics, MBRO detectors can also be utilized to study geoneutrinos, astrophysical neutrinos and proton decay. We propose to start a U.S. R&D program to identify, quantify and fulfill the key challenges essential for the success of MBRO experiments.

*Submitted to the Snowmass 2013 Proceedings

Contents

1	Introduction	2
2	Medium-baseline reactor neutrino experiments resolving MH	4
2.1	MH signal in MBRO experiments and challenges	4
2.2	Mass hierarchy sensitivity study	6
2.2.1	The χ^2_{min} comparison method resolving MH	6
2.2.2	Background assumptions	6
2.3	Impact of detector energy responses	7
2.4	Expected sensitivity of MBRO experiments to MH	8
2.5	Reactor flux uncertainty impact	10
2.6	A dual detector design with ratio methods	11
3	Precision measurements and synergy with $\nu_\mu/\bar{\nu}_\mu$ disappearance experiments	11
3.1	Precision oscillation parameter measurement	11
3.2	Synergy with $\nu_\mu/\bar{\nu}_\mu$ disappearance experiments in MH determination	12
4	Performance requirements of MBRO LS detectors and R&D	13
4.1	Summary of the unprecedented challenges in MBRO experiments	13
4.2	PMT system study	14
4.3	Liquid scintillator study	15
4.4	Front-end and trigger electronics	16
4.5	Detector energy response calibration	17
5	Other potential physics topics	18
6	Summary and conclusions	18

1 Introduction

The precise measurement of $\sin^2 2\theta_{13}$ by the current generation of short-baseline reactor neutrino experiments [1, 2, 3] has provided a unique opportunity to determine the neutrino mass hierarchy (MH) in a medium-baseline reactor neutrino oscillation (MBRO) experiments [4, 5, 6, 7, 8, 9, 10, 11, 12, 13, 14]. By employing large liquid-scintillator (LS) detectors at distances greater than ~ 30 km from nuclear reactors, we can observe the oscillation signals driven by both the solar mass-squared splitting (Δm_{21}^2) and the atmospheric mass-squared splitting (Δm_{32}^2) in the antineutrino energy spectrum [11]. The oscillation resulted from the atmospheric mass-squared splitting manifests itself in the energy spectrum as multiple cycles which shift in the opposite directions for inverted hierarchy (IH) and normal hierarchy (NH), as shown in the following formula,

$$\begin{aligned}
 P_{\bar{\nu}_e \rightarrow \bar{\nu}_e} &= 1 - \sin^2 2\theta_{13} (\cos^2 \theta_{12} \sin^2 \Delta_{31} + \sin^2 \theta_{12} \sin^2 \Delta_{32}) - \cos^4 \theta_{13} \sin^2 2\theta_{12} \sin^2 \Delta_{21} \quad (1) \\
 &= 1 - 2s_{13}^2 c_{13}^2 - 4c_{13}^2 s_{12}^2 c_{12}^2 \sin^2 \Delta_{21} + 2s_{13}^2 c_{13}^2 \sqrt{1 - 4s_{12}^2 c_{12}^2 \sin^2 \Delta_{21}} \cos(2\Delta_{32} \pm \phi),
 \end{aligned}$$

where $\Delta_{21} \equiv \Delta m_{21}^2 L/4E$, $\Delta_{32} \equiv \Delta m_{32}^2 L/4E$, in which L is the baseline and E is the antineutrino energy, and

$$\sin \phi = \frac{c_{12}^2 \sin 2\Delta_{21}}{\sqrt{1 - 4s_{12}^2 c_{12}^2 \sin^2 \Delta_{21}}}, \quad \cos \phi = \frac{c_{12}^2 \cos 2\Delta_{21} + s_{12}^2}{\sqrt{1 - 4s_{12}^2 c_{12}^2 \sin^2 \Delta_{21}}}.$$

In contrast to electron-neutrino appearance experiments such as the Long Baseline Neutrino Experiment (LBNE) and the Long Baseline Neutrino Oscillation Experiment (LBNO) [15, 16, 17], which have to take into account the effects from δ_{CP} , MBRO experiments are free of any effects due to the unknown δ_{CP} phase. The amount of the shift in the neutrino energy spectrum due to different MH is characterized by the ratio of $\Delta m_{21}^2/\Delta m_{32}^2$, which is about 0.03, therefore to make a meaningful measurement of the neutrino MH effect in MBRO experiments, one needs excellent energy resolution and well-calibrated detector energy response. Recent studies show that with a detector energy resolution $\sim 3\%/\sqrt{E(\text{MeV})}$ * and energy non-linearity measured to sub-1% over the entire reactor antineutrino energy spectrum, a $\Delta\chi^2 = 16^\dagger$ measurement can be made in 5 years with an exposure of 800 kt-GW_{th} per year at a baseline of $\sim 60\text{km}$ [18]. Such high performance detectors can also make precise measurements of $\sin^2 2\theta_{12}$, Δm_{21}^2 and Δm_{32}^2 to sub-percent level. In addition, they are excellent detectors for studying other important physics topics such as geoneutrinos, solar neutrinos, atmospheric neutrinos, and proton decay. Together with the improving $\sin^2 2\theta_{13}$ precision by the current generation short-baseline reactor neutrino experiments, it will enable a future direct unitarity test of the PMNS matrix to $\sim 1\%$ level. It can also help to constrain the allowed region in the phase space of $\langle m_{\beta\beta} \rangle$ vs. m_{light} , the lightest neutrino mass, and provide more precise absolute neutrino mass constraints should the neutrinoless double beta decay experiments observe any signals [19]. If we are lucky enough to witness a supernova within 10 kpc during the experiment's live time, we would expect to record about 6000 supernova neutrinos with accurately measured energy and time profile for a 20kt detector.

A MBRO experiment at Jiangmen Underground Neutrino Observatory (JUNO) in China has been proposed to measure the neutrino mass hierarchy [18]. The proposed detector contains about 20kt of liquid scintillator (LS) under a $\sim 700\text{m}$ overburden and will be located $\sim 60\text{km}$ from two nuclear power plants with a total power of $\sim 36\text{GW}_{th}$ currently under construction. This experiment is expected to record $\sim 10^5$ inverse beta decay (IBD) events in five years. Another MBRO experiment named RENO-50 has been proposed in South Korea. RENO-50 proposes to build a 18kt LS detector at a distance of 47km from the current RENO reactor complex [20].

There are many challenges to such an experiment. In addition to the requirements of a very large detector volume and very good energy resolution, very precise energy calibration is also critical for the experiment. Excellent energy resolution can be achieved with maximal photocathode coverage in the detector, enhanced scintillation light yield as well as long scintillator light attenuation length. Calibration of such a large detector to the required precision is non-trivial. The energy scale requirements demand the deployment of a comprehensive suite of calibration sources and making detector response measurement to sub-1% level, which pose great challenges in engineering as well as detector simulation. These challenges require an intensive, target oriented R&D program. US groups with extensive experiences in solar, reactor and atmospheric neutrino experiments such as Super-K, SNO, KamLAND and Daya Bay are in an excellent position to undertake such a R&D program for MBRO experiments. In this paper, we explore the rich physics potential of MBRO experiments based on the realistic performance obtained or extrapolated from the past experiments. By quantifying the requirements, we are able to identify the key issues that the U.S. R&D program needs to address. The paper is organized as follows. In Sec. 2, we discuss the nature of the MH signals in massive LS detectors and evaluate the sensitivities based on the current proposals and inputs from the existing reactor neutrino experiments. Precision oscillation parameter measurements are discussed in Sec. 3. Based on our sensitivity studies and proposed physics goals, we identify the key detector performance requirements and discuss their realization and possible R&D plans in Sec. 4. Physics potential other than neutrino oscillation physics is covered in Sec. 5. We then give our summary and conclusions on

*Besides the dominant term due to photo-electron statistical fluctuation, energy resolution expression also includes non-uniformity and noise contributions. The overall resolution needs to be better than 3% at 1MeV.

†See Sec. 2.2 on the relationship between $\Delta\chi^2$ values and confidence levels for MH determination.

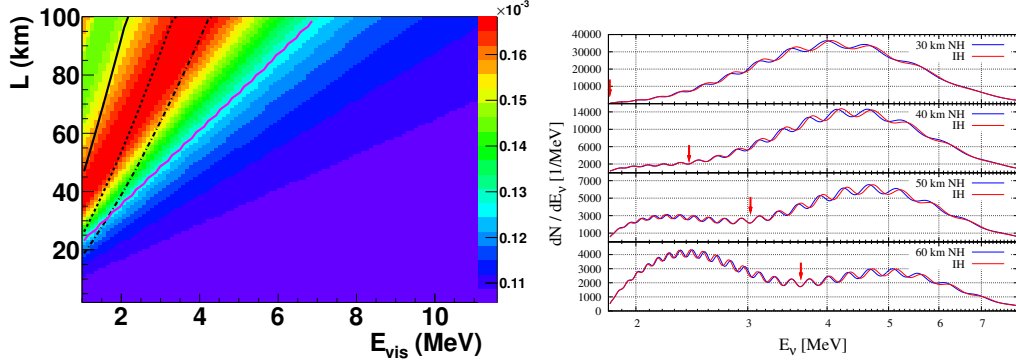


Figure 1: Left: the effective mass-squared difference shift Δm_ϕ^2 as a function of baseline and visible prompt energy $E_{vis} \approx E_\nu - 0.8 \text{ MeV}$. Right: the comparison of energy spectra between NH and IH at different baselines. Arrows mark the location where $\Delta m_\phi^2 = 0$.

MBRO experiments and possible U.S. roles in such experiments.

2 Medium-baseline reactor neutrino experiments resolving MH

2.1 MH signal in MBRO experiments and challenges

As has been pointed out in the previous section, it is plausible to determine the MH from the energy spectrum of detected reactor antineutrinos at suitable distances from a nuclear reactor [4, 5, 6]. As shown in Eq. 1, the MH dependence comes solely through the phase shift ϕ , which takes a plus sign for NH and minus sign for IH. The value of ϕ depends on the neutrino energy and is in general small ($\sim 5\%$ of Δm_{32}^2) in the energy range of the reactor neutrinos (1.8 - 10 MeV). To resolve this small spectrum difference between the two MH hypotheses, it requires both large statistics and good control of systematics.

Ref. [7, 9, 10, 11, 21] show that energy resolution better than $\sim 3\%/\sqrt{E(\text{MeV})}$ is needed in order to resolve the difference between NH and IH. This can be easily understood from the left panel of Fig. 1, which shows the energy and baseline dependent phase shift of ϕ . In principle, the MH can be resolved by comparing the measured effective mass-squared difference $\Delta m_{32}^2 \pm \Delta m_\phi^2/2$ at low energy ($\sim 3 \text{ MeV}$) vs. that at high energy ($\sim 6 \text{ MeV}$). Here, we have defined $\Delta m_\phi^2 \equiv 4E\phi/L$ based on Eq. 1. For NH, the effective mass-squared difference at low energy will be larger than that at high energy and vice versa for IH. However, at low energy, since the L/E is large, a poor energy resolution will smear the oscillation signals corresponding to the atmospheric oscillation (Δm_{32}^2), leading to difficulties for measuring the true oscillation frequency at low energy region.

Besides the challenges held in the energy resolution, uncertainties in the value of Δm_{32}^2 could result in the degeneracy of NH and IH that makes it impossible to measure MH. Fig. 2 shows comparison of the visible energy spectra of the inverse beta decay (IBD) events between NH and IH at a distance of 60km. The left panel is the ideal case and the difference between NH and IH is visible across the entire spectrum. Due to the Δm_{32}^2 uncertainty, as shown in the middle panel of Fig. 2, degenerated oscillation probabilities significantly reduce the spectrum difference between different MHs. The situation becomes worse when statistical fluctuations are included, as shown in the right panel of Fig. 2. To overcome this challenge, we need more accurate independent measurement of Δm_{32}^2 as pointed out in Ref. [18, 21]. Reference [18] shows that, under different set of assumptions, with the possible improvement on Δm_{32}^2 to 1.5% (T2K, NO ν A), the MH sensitivity can be increased to $\Delta\chi^2 \cong 20$ in 6

year running time.

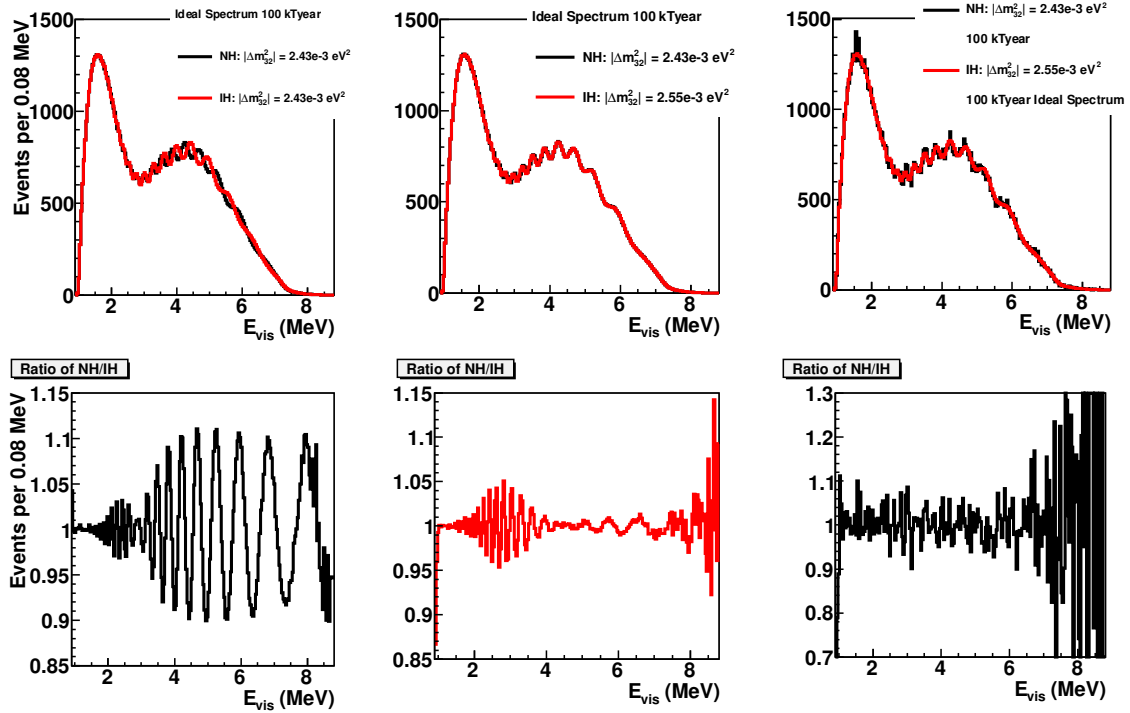


Figure 2: Comparison of the energy spectra of the positron signal under different assumptions for NH and IH cases. The uncertainty in Δm_{32}^2 was assumed as $\sim 0.13 \times 10^{-3} eV^2$ in Summer 2012 when the paper was published.

The baseline of MBRO experiments needs to be greater than ~ 30 km in order to resolve the MH signal reliably. This is illustrated in Fig. 1, taken from Ref. [21] (left) and Ref. [13] (right). From the left panel of Fig. 1, for baselines less than ~ 30 km, Δm_{ϕ}^2 is rather uniform across the entire IBD spectrum and the current uncertainty in Δm_{32}^2 can easily absorb it thus it is impossible to distinguish between NH and IH. For baselines greater than ~ 30 km and close to ~ 60 km, the solar oscillation suppression of the reactor flux is near its maximum and energy dependent Δm_{ϕ}^2 makes the MH effect more visible. The right panel of Fig. 1 shows the same observation from the spectrum perspective, the opposite phase shifts between the low and high energy regions only appear when baselines are greater than ~ 30 km.

The needs of good energy resolution and large number of free proton targets for IBD antineutrino reaction make liquid scintillator (LS) the best choice for MBRO experiments. However, LS has a notorious property: non-linear energy response caused by energy quenching and Cherenkov radiation. Combined with possible electronic non-linear effect, inaccurate energy calibration could potentially cause degenerated energy spectra between different MHs if the energy reconstruction is biased in the following non-linear fashion,

$$E_{rec} = \frac{2|\Delta' m_{32}^2| + \Delta m_{\phi}^2(E_{\bar{\nu}_e}, L)}{2|\Delta m_{32}^2| - \Delta m_{\phi}^2(E_{\bar{\nu}_e}, L)} E_{real}. \quad (2)$$

Here E_{rec} is the reconstructed energy and E_{real} is the true energy. $|\Delta' m_{32}^2|$ represents a different Δm_{32}^2 best-fit value obtained from the observed energy spectrum allowed by its current uncertainty. It has

been illustrated in Ref. [21] that with the allowed uncertainty $\delta(\Delta m_{32}^2) = 0.13 \times 10^{-3} eV^2$, to break the degeneracy, energy non-linearity needs to be understood to the sub percent level. The current generation of large LS detectors can achieve a precision of $\sim 2\%$. This requirement can be relaxed if the uncertainty in Δm_{32}^2 get improved.

In addition to the most critical requirements on energy resolution and energy response, there are other challenges in MBRO experiments, such as backgrounds, reactor core distributions and event statistics. We will discuss these factors with the sensitivity study in the following sections.

2.2 Mass hierarchy sensitivity study

2.2.1 The χ_{min}^2 comparison method resolving MH

To study the physics sensitivity of MH determination in MBRO experiments, a χ^2 is constructed using the pull method to do a model comparison between NH and IH as follows,

$$\chi^2 = \sum_{i=1}^N 2 \cdot (N_i^{exp} - N_i^{obs} + N_i^{obs} \cdot \log(N_i^{obs}/N_i^{exp})) + \chi_{penalty}^2, \quad (3)$$

where N_i^{obs} is the number of observed IBD events in energy bin i given one of MH is true and N_i^{exp} is the expected number of IBD events in bin i assuming either NH or IH. The penalty component $\chi_{penalty}^2$ includes systematic constraints and any *a priori* knowledge on oscillation parameters from other experiments. The best-fit minimal χ^2 difference between the two MH hypotheses is defined as: $\Delta\chi^2 \equiv \chi_{min,IH}^2 - \chi_{min,NH}^2$. Naturally, a positive $\Delta\chi^2$ indicates the NH model is preferred by the data over the IH model as the better model has smaller χ_{min}^2 .

For continuous quantities that can be approximated by normal distributions, the $\sqrt{|\Delta\chi^2|}$ in the unit of standard Gaussian deviation σ is commonly used as the confidence level (C.L.). However, as pointed out in Ref. [22], due to the discrete nature of MH, the square root rule does not apply any more in setting the C.L. for MH measurement. The proper relation between $\Delta\chi^2$ and C.L. for a simple example is shown in Fig. 3. The new rule requires a greater $\Delta\chi^2$ to reach the same C.L. This fact has been confirmed in Ref. [13, 14]. For convenience, we will still use $\Delta\chi^2$ as the quantity representing sensitivity. However, we should keep in mind that the C.L. vs $\Delta\chi^2$ relation for MH measurement has been modified. This is a special case of the Feldman-Cousins method when the distribution of the measured quantity is better approximated by a 2-value binomial distribution. Based on this finding, $\Delta\chi^2$ has to be ~ 100 to reach the 5σ discovery level, well beyond the sensitivity of any current MBRO experiment proposals. To reach the 3σ strong indication level, a MBRO experiment needs to be able to reach $\Delta\chi^2 \sim 36$, which is still very difficult based on current predictions.

2.2.2 Background assumptions

We have taken the background spectra from Daya Bay or theoretical calculations and extrapolated the background rates based on the KamLAND results [1, 2, 23]. The backgrounds we have considered include:

- Accidental background

With five years of run time, we expect ~ 3000 events from the accidental background and its prompt signal spectrum is assumed to be the same as the one in Daya Bay. Since the prompt signal spectrum can be directly measured with high precision, we assume the accidental background rate uncertainty is negligible.

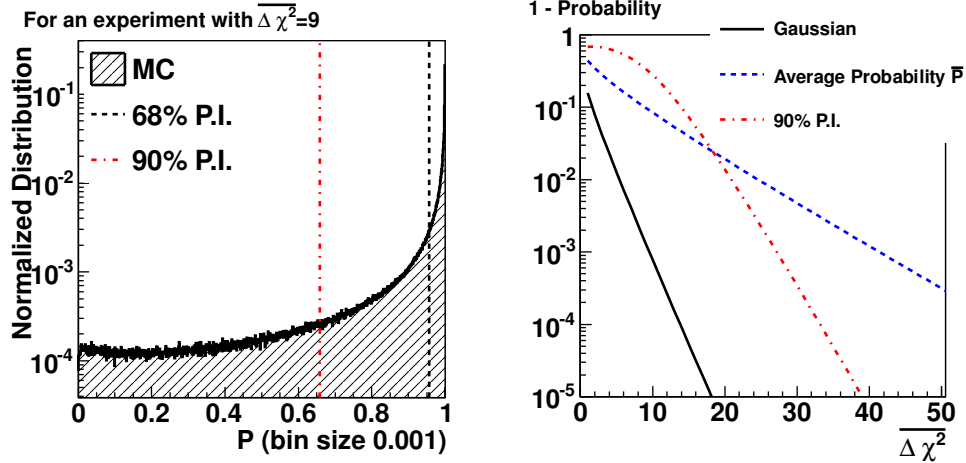


Figure 3: The left panel shows the distribution of $P(\underline{NH}|x) = P(NH|\Delta\chi^2)$ over the population of potential data x that arises from an experiment with $\overline{\Delta\chi^2} = 9$ where the truth is NH. The mean of this distribution is 90.14%. Lower bound of the 68% and 90% probability intervals are plotted. That is, 68% (90%) of the data x would yield a $P(NH|x)$ that falls to the right of the dash-dotted (dashed) line. These two lines are also commonly referred as the 32th and the 10th percentile. The right panel plots several sensitivity metrics (subtracted from 1 for clarity), against $\overline{\Delta\chi^2}$ that ranges from 1 to 50. Note that all the lines are decreasing because higher values of $\overline{\Delta\chi^2}$ corresponds to more sensitive experiments. This is done for three different criteria: the Gaussian interpretation (derived from the one-sided p-value with one degree of freedom), \bar{P} and $P_{T=NH}^{90\%}$. The Gaussian interpretation is seen to be over-optimistic in describing the ability of the experiment to differentiate the two hypotheses.

- ${}^9\text{Li}/{}^8\text{He}$ background
We expect ~ 550 events. A 30% rate uncertainty in the ${}^9\text{Li}/{}^8\text{He}$ background is assumed. We use the theoretical spectrum in this study.
- Fast neutron background
We expect ~ 400 events. The energy spectrum is assumed to be flat and a 50% rate uncertainty is assumed.
- ${}^{13}\text{C}(\alpha, n){}^{16}\text{O}$ background
We expect ~ 6300 events. The energy spectrum is assumed to be the same as that measured in Daya Bay. A 20% rate uncertainty is assumed.
- Geoneutrino background
We expect ~ 3600 events. A 10% rate uncertainty is assumed. We use the theoretical spectrum in this study.

For all the backgrounds above, we neglect uncertainties in the spectral shape.

2.3 Impact of detector energy responses

In order to study the effect of non-linear energy scale uncertainties, we have assumed 3 types of energy models:

1. Model I:

The non-linear model set by Eq. 2, also shown as the red curve in Fig. 4. We have assumed NH as the true MH and the energy scale uncertainty of 1%.

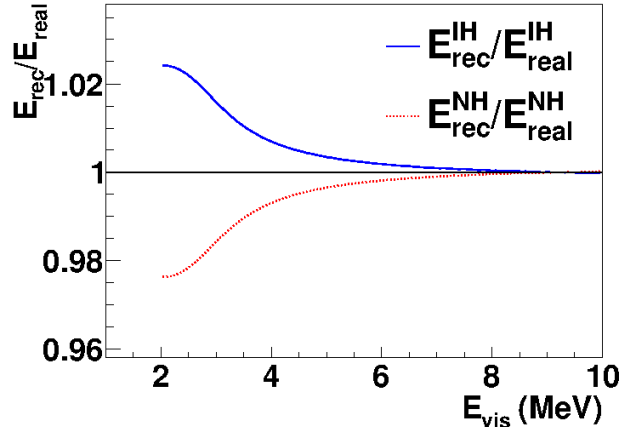


Figure 4: Energy non-linearity models that can cause degeneracy when the true MH is NH (red) and IH (blue). See text for more explanations.

2. Model II:

A linear shift in the absolute energy scale uncertainty of 1%, $\sigma_{scale} = 1\%$.

3. Model III:

The current preliminary Daya Bay non-linear model, which is a combined model based on multiple nearly independent models. These multiple energy models are constructed with different emphases of the calibration and control data. The energy scale uncertainty is at $\sim 1\%$ level across the IBD spectrum. This approach provides the flexibility in the functional form of the non-linearity model. For details, see Ref. [24].

With the above 3 different energy scale models, we first perform a baseline scan. Fig. 5 shows the sensitivity evolution with respect to the baseline. Depending on the choice of the energy response models, optimal baseline varies between 40km and 60km, which is consistent with the findings of other groups.

Next, we study the effect of energy resolution on the sensitivity. For energy resolution, we choose the following generic model,

$$\frac{\Delta E}{E} = \sqrt{a^2 + \frac{b^2}{E} + \frac{c^2}{E^2}}. \quad (4)$$

Where ΔE is the energy resolution at a total visible energy E , a is due to the energy leakage and detector non-uniformity, b is the term that depends on the photo-electron (PE) statistics, and c is due to background and noise. We have assumed $a = 0.7\%$ and $c = 0.85\%$, which are extrapolated from the performance of the Daya Bay and KamLAND detectors. Fig. 6 shows the sensitivity dependence on the statistical uncertainties in the total number of PEs. As we can see, the sensitivity drops dramatically once the PE uncertainty is greater than $\sim 3\%$ for Model 2 and 3. For the designed Model I, the turning point is even lower, at $\sim 2.5\%$.

2.4 Expected sensitivity of MBRO experiments to MH

Fig. 7 shows the sensitivity evolution with respect to exposure. We see that with the designed degeneracy energy scale (energy model I), the $\Delta\chi^2$ can reach ~ 10 in a 5 year run, which is a very pessimistic situation. With the current preliminary Daya Bay energy scale model (energy model III) and uncertainty, the final $\Delta\chi^2$ could reach ~ 14 , which is about 2σ ($\Delta\chi^2 \sim 16$) quoting the conventional

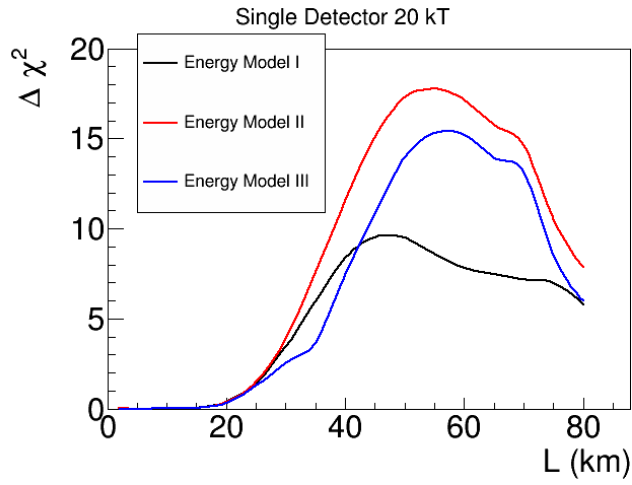


Figure 5: MH sensitivity evolution with respect to different baseline choices under different energy response assumptions.

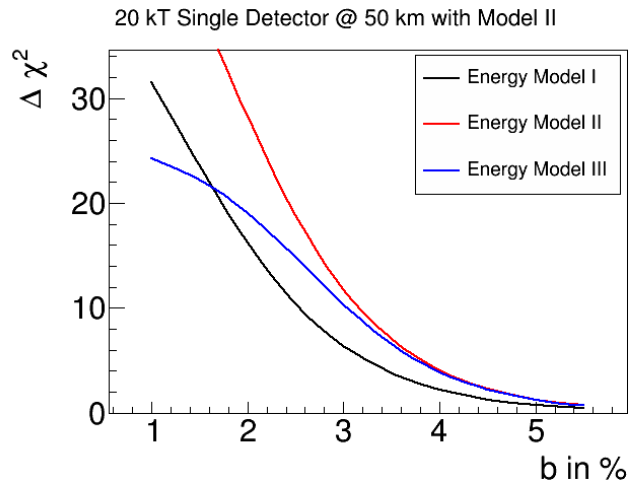


Figure 6: MH sensitivity as a function of the b term in the resolution function (Eq. 4) for the 3 different energy scale models.

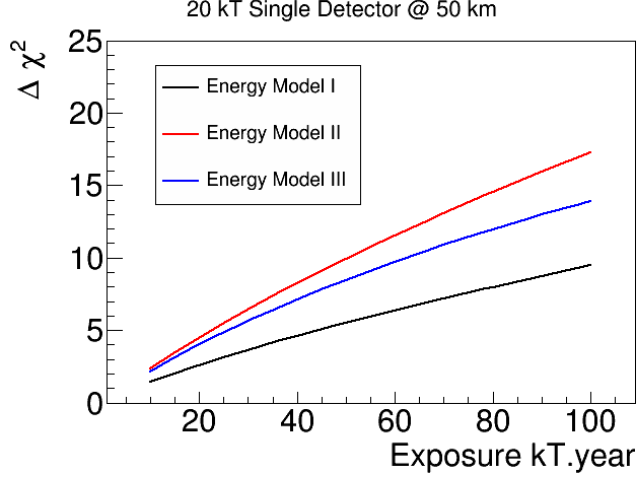


Figure 7: The time evolution of $\Delta\chi^2$ with respect to exposure

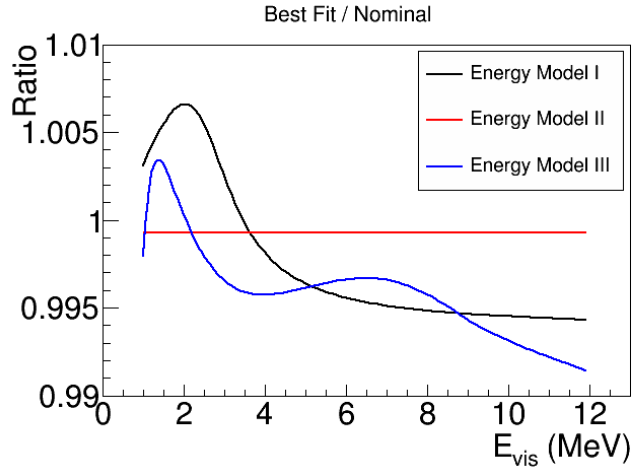


Figure 8: Fitted energy model at the $\Delta\chi^2$ minimum for three energy models.

frequentist statement on the C.L. of the measurement. With a linear energy scale uncertainty model (energy model II), the 5-year $\Delta\chi^2$ could reach ~ 17 , which corresponds to $\sim 2\sigma$ C.L. ($\Delta\chi^2 \sim 16$).

As can be seen, the MH sensitivity strongly depends on the choice of the non-linearity model (10 vs. 14 vs. 17 for model I, II, and III, respectively). Fig. 8 shows the fitted energy model at the $\Delta\chi^2$ minimum for these three models. Therefore, it is important to have a good understanding of the energy response, at least the functional form of the energy model. The latter can also be viewed as a good constraint on the relative energy scale between the low and high energy regions.

2.5 Reactor flux uncertainty impact

The knowledge of the reactor spectrum plays an important role to obtain the absolute energy model, which would then help to increase the MH sensitivity in MBRO experiments. This is due to that reactor flux is correlated between energies[25, 26]. In this study, we have used the correlation matrix based on the Daya Bay reactors. Table 1 shows the improvements on MH sensitivity as reactor flux uncertainty is reduced. Smaller reactor flux uncertainties can be achieved by employing near detectors. For example, RENO-50 is planning to use the current RENO detectors as its near detectors[20].

Table 1: Improvements in MH sensitivity with 100kt exposure as a function of improvement in the reactor flux.

Uncertainty improvement	$\Delta\chi^2$ (Model I)	$\Delta\chi^2$ (Model II)	$\Delta\chi^2$ (Model III)
Current $\sim 3\%$	9.5	17.3	13.9
Improve by a factor of 2	11.5	21.7	18.4
Improve by a factor of 3	12.1	23.2	19.9
Improve by a factor of 4	12.4	23.8	20.5
Improve by a factor of 5	12.6	24.1	20.9

Table 2: Improvement in MH sensitivity for the degeneracy non-linearity model, Model I, with different second detector options and under different energy scale uncertainty improvements

2nd Detector	$\Delta\chi^2$	$\Delta\chi^2$ ($\sigma_{scale}/4$)
20kt at 53km	4.2	14.3
0.1kt at 2km	4.9	11.5
5kt at 30km	10.3	13.6

2.6 A dual detector design with ratio methods

With two detectors, one can form ratios between these two detectors, so that the uncertainties from the reactor spectrum are largely canceled[‡]. However, as shown in Ref. [21], using ratios directly would be more sensitive to the uncertainty in the energy model, as the constraint from the knowledge of the reactor spectrum is not being used. This is also true for the proposed Fourier transformation methods [7, 10, 11]. On the other hand, Ref. [27] showed that by placing a second functionally identical detector at ~ 30 km baseline, the energy non-linearity requirement can be greatly relaxed. This is because the MH-dependent oscillation patterns are different at the two baselines, therefore a single “wrong” non-linearity can not fit both detectors if the two detectors have highly correlated energy responses. In our sensitivity calculation, we find that such a configuration of detectors does improve the sensitivity significantly. Our results are shown in Table. 2. In our study, we have assumed the second detector’s energy scale is fully correlated with the far detector. With the assumed energy scale uncertainties based on the current Daya Bay preliminary results, a second detector at $L=30$ km can significantly improve the MH sensitivity with the ratio method. In order to reach the same sensitivity of the dual detector configuration, single detector setup has to be able to reduce the energy scale uncertainties significantly.

3 Precision measurements and synergy with $\nu_\mu/\bar{\nu}_\mu$ disappearance experiments

3.1 Precision oscillation parameter measurement

With ~ 40 detected reactor neutrino events per day, and the multiple oscillation cycles in the energy range of reactor neutrinos, it is estimated [18] that Δm_{21}^2 , Δm_{31}^2 and $\sin^2 \theta_{12}$ can be measured to a precision of $\sim 0.6\%$. It enables a future direct unitarity test of the PMNS matrix ($|U_{e1}|^2 + |U_{e2}|^2 + |U_{e3}|^2 \stackrel{?}{=} 1$) to a sub-percent level [28]. Our study with background assumptions listed in Sec. 2.2 shows that sub-percent precision oscillation parameter measurement is plausible. Fig. 9 shows the precisions of measuring oscillation parameters at different baseline values. It is not surprising that

[‡]The assumption here is not to take the theoretical uncertainty estimations of reactor spectrum as granted.

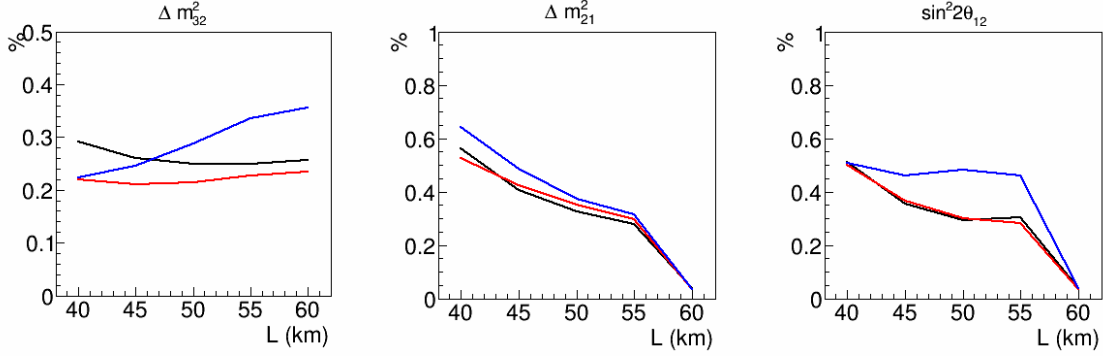


Figure 9: Projected precision oscillation parameter measurement uncertainties at different baselines. Black: Energy Model I; Red: Energy Model II; Blue: Energy Model III

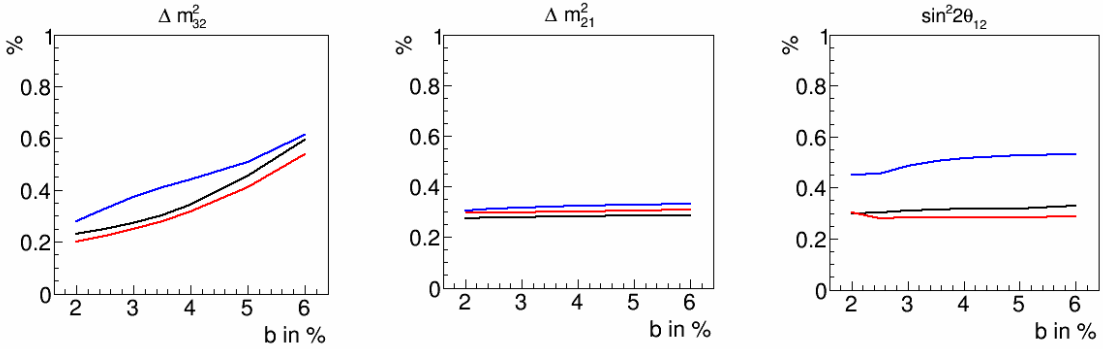


Figure 10: Projected precision oscillation parameter measurement uncertainties at different energy resolution performances. Black: Energy Model I; Red: Energy Model II; Blue: Energy Model III

the best baseline for measuring solar sector parameters happens at the solar oscillation maximum, which is $\sim 60\text{km}$ for the energy range of reactor flux. On the other hand, the Δm_{32}^2 precision does not depend on the baseline much as long as there are multiple oscillation cycles in the survival spectrum. However, the precision to Δm_{32}^2 decreases quickly as energy resolution is over $\sim 3\%/\sqrt{E(\text{MeV})}$ as shown in Fig. 10. As the solar scale oscillation spans over the entire spectrum at the distance of $\sim 60\text{km}$, the energy resolution has little impact to the solar oscillation parameter precisions.

3.2 Synergy with $\nu_\mu/\bar{\nu}_\mu$ disappearance experiments in MH determination

As the uncertainty in Δm_{32}^2 gets improved in coming years from $\nu_\mu/\bar{\nu}_\mu$ beam experiments like NO ν A and T2K, the sensitivity of MBRO experiments also gets improved significantly as shown in Ref [18]. While MBRO experiments are utilizing vacuum oscillation of reactor antineutrinos to measure MH, experiments like PINGU (Precision IceCube Next-Generation Upgrade), ORCA (Oscillation Research with Cosmics in the Abyss) and INO (India Based Neutrino Observatory) are utilizing resonant oscillation due to matter effect of atmospheric neutrinos to achieve the same goal [29, 30]. As pointed out in Ref. [31], due to the unprecedented challenges in both types of experiments, each type alone might not be able to reach the discovery sensitivity. However, as the two types of experiments are constraining the key oscillation parameter $|\Delta m_{32}^2|$ for MH resolution from different perspectives, they are complementary thus combined data can increase the sensitivity to MH. Fig. 11 taken from Ref. [31] shows the $\Delta\chi^2$ for PINGU, JUNO (Daya Bay II) as well as combined PINGU+JUNO+T2K as a

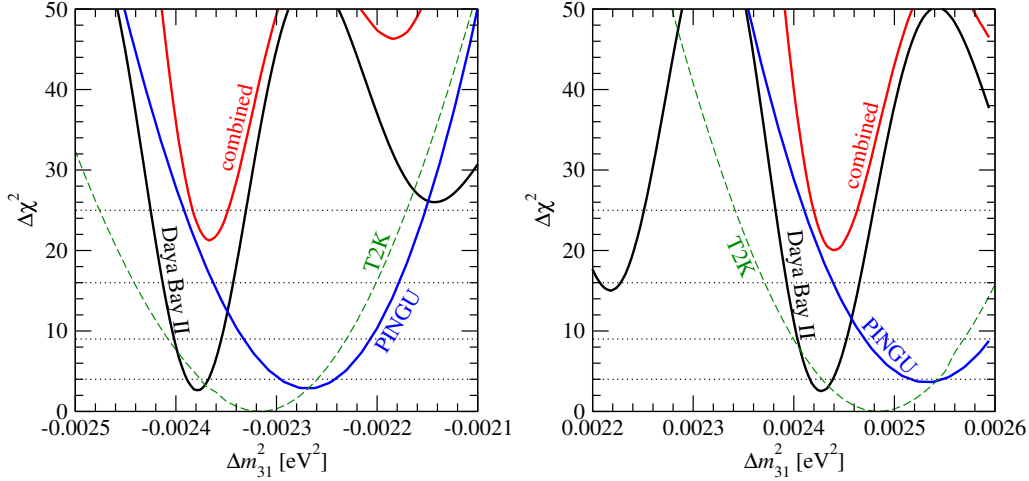


Figure 11: Combined JUNO, T2K and PINGU data enhancing the sensitivity to the MH. Left panel assumes NH as the true MH and the right panel assumes IH.

function of Δm_{31}^2 [§] with the wrong MH assumed.

4 Performance requirements of MBRO LS detectors and R&D

4.1 Summary of the unprecedented challenges in MBRO experiments

Based on the existing studies and our studies presented in previous sections, we can summarize the major challenges of MBRO experiments as follows,

- Statistics challenge.

With 40 GW_{th} reactor power and a detector of 20 kt LS at a baseline of 60 km, in 5 year running time, a total of $\sim 10^5$ inverse beta decay events can be collected. Monte Carlo simulation shows that the χ^2 difference between the two MH hypotheses ($\Delta\chi^2$) fits for an Asimov data set can reach ~ 25 assuming a energy resolution of $\sim 2.6\%/\sqrt{E(\text{MeV})}$ and perfect systematics [21]. However, based on MC, the average probability to determine the correct MH is determined to be 98.9% [21, 22], not to the conventionally believed 5σ level due to the different statistics followed by MH. Thus in MBRO experiments, to resolve MH with high CLs, large statistics is needed, which can only be achieved with massive detectors together with powerful reactors. One of the major challenges in ensuring sufficient statistics lies in the construction of a $>10\text{kt}$ LS detector, which is unprecedented.

- Reactor core distribution and site selection.

MBRO experiments need multiple reactors to increase the statistics. However, if the multiple baselines differ by 1~5km, the MH sensitivity can be greatly reduced due to the cancellation effect [32, 18]. Also considering the backgrounds produced by the cosmic muons, the site needs to have an overburden $>\sim 500\text{m}$ (rock). JUNO has identified the Jiangmen site, which is $\sim 60\text{km}$ away from Yangjiang and the Taishan reactor complexes, to meet those criteria [32]. Suitable site locations are essential for the success of MBRO experiments.

[§]The choice of $|\Delta m_{31}^2|$ or $|\Delta m_{32}^2|$ does not change the MH discussion as $|\Delta m_{31}^2| \gg \Delta m_{21}^2$. It is only a change of the reference mass eigenstate.

- Energy resolution.

This is the well-recognized unprecedented challenge in large LS detectors. We have showed that a $< \sim 3\% / \sqrt{E(\text{MeV})}$ energy resolution is needed for the experiment, otherwise the fine structure of the oscillation pattern due to MH is smeared out, especially at low energy $< \sim 4$ MeV. To achieve such a good energy resolution, it requires dedicated R&D programs to address the following items [33, 32]:

- High photo-cathode coverage of the detector, $\sim 80\%$
- Photomultiplier tubes (PMT) with high collection efficiency and quantum efficiency (QE), $\sim 35\%$
- Highly transparent LS with attenuation length of $\sim 35\text{m}$ (for the dimension of a 20kt LS detector)
- High light yield LS ($\sim 1.5 \times$ photon yield of KamLAND LS)

- Energy non-linearity.

As shown in Ref. [21], an unrecognized detector energy non-linearity could fake one MH as the other. Our sensitivity study in Sec. 2 shows that a degeneracy caused energy scale bias could greatly reduce the sensitivity. Therefore, to ensure the MH's discovery potential, the non-linearity of energy scale (E_{rec}/E_{real}) needs to be understood to a fraction of 1% in a wide range of energy spectrum. This requirement should be comparable to the current state-of-art 1.9% energy scale uncertainty from KamLAND [34]. The non-linearity could come from different origins such as scintillation quenching, Cherenkov light, electronics, reconstruction non-uniformity, etc. An extensive calibration program is crucial for the experiment. Such a calibration program requires multiple energy calibration points inside the full fiducial volume of the detector. Multiple types of sources are desired, in particular positron sources to cover the wide range of the IBD spectrum to eliminate the potential degeneracy caused non-linearity. A dedicated R&D program is definitely needed.

4.2 PMT system study

There are two major challenges for the PMT system in MBRO experiments. One challenge of the PMT system is to ensure the mechanical safety and the other is related to performance: low dark noise, high collection and quantum efficiencies, and high photocathode coverage are needed. We consider the following R&D items are necessary:

- PMT safety.

Large format semi-hemispherical PMTs are leading candidates for the detector. Following the Super-K incident, the ability of PMTs to withstand hydrostatic pressure and control the propagation of PMT implosion impact has become critical issues for any large detector readout by PMTs [35, 36]. PMT glass in liquid is known to undergo stress-induced corrosion. Even with good quality control, microscopic cracks in the PMT glass act as concentrators of stress. Once the concentrated stress exceeds the strength of glass, it will lead to cracking and failure (implosion). High photocathode coverage means high density of PMTs in the detector. In case of PMT implosion, the propagation of the shock waves to the surrounding PMTs could cause chain action. Therefore, a systematic study to contain the implosion impact is needed to prevent the disaster. Based on our prior experience, a number of simulation studies must be performed to address PMT mechanical performance.

- Collection and quantum efficiency enhancement.

It is critical for the LS detector to reach $\geq 80\%$ photocathode coverage to control the energy

resolution better than $\sim 3\%/\sqrt{E(\text{MeV})}$. Due to geometric constraints, the design is quite challenging. Thus other means to enhance the detection efficiency are necessary. We have considered the following two options for this purpose:

- One option we have considered is to add Winston cones should the conventional PMTs are used by MBRO experiments. Winston cones have been utilized to increase light detection efficiency using specular reflection from metallic, mirror-like ellipsoidal surfaces and funneling light toward PMT photocathode surfaces. This is an attractive option to collect light lost in the spaces between PMTs. Mechanical designs need to be developed in order to accommodate Winston cones together with PMT mounting schemes.
- PMTs are susceptible to local magnetic field, such as the Earth’s field of 0.4-0.5 Gauss. The magnetic field can reduce the PMT collection efficiency as well as causing nonuniform response of PMTs to signals [37]. Therefore, we need to R&D various PMT magnetic field shielding methods to create ideal working conditions for PMTs.
- PMT performance characterization. A new kind of PMT is being designed for JUNO using micro-channel plates (MCPs) for PE collection and amplification. The performance of new PMT needs to be fully studied.

4.3 Liquid scintillator study

All studies from other groups and our group have shown it is absolutely critical to reach energy resolution to less than 3% at 1 MeV. One of the key elements in reaching the unprecedented energy resolution in such a LS detector is higher photon yield. The typical proposed dimensions are $\sim 35\text{m}$ in diameter for JUNO and $\sim 25\text{m}$ in diameter and height for RENO-50. Thus LS transparency needs to reach $\sim 30\text{m}$ level at least. As we need large statistics to resolve the MH, the aging rate of the LS to be sufficiently low so transparency can stay at the acceptable level for at least 5 years.

The R&D tasks of necessity are therefore:

- Purification of scintillator and fluor. We need to control scintillator impurities (e.g. non-radioactive chemical species that adversely affect optical properties) and develop methods to remove and assay residual radioactive contaminants, mainly from the naturally occurring ^{238}U and ^{232}Th decay chains. Typical liquid scintillator purchased from industry has an attenuation length of $\sim 10\text{m}$ with most impurities introduced during the production process. The best optical attenuation length achieved for a liquid scintillator is $L_{attn} \sim 20\text{m}$ at 430nm (LAB, after extensive purifications). Several technologies, such as vacuum distillation (SNO+, KamLAND, Borexino) or column extraction (industrial, petrochemical) can improve optical transmission. A combination of extraction column during the distillation phase might further improve the solvent. Another approach is the use of high-purity starting materials (e.g. nD instead of MO for LAB) as the feedstock for scintillator production such that cleaner liquid can be obtained. Other means of purification by separation resin or solvent washing should be tested. For instance, PPO (known to be a dirty material) can be cleaned by water-washing, recrystallization or solvent-distillation.
- Search for a new scintillator that can be mass produced. Pseudocumene was selected by early experiments (Palo Verde, CHOOZ) due to its large scintillation output; however, it has a low flash point and poor material compatibility, thus a second, non-aromatic solvent (mineral oil or n-dodecane) has to be added to offset those effects. Such mixtures degrade the light-yield and complicate the scintillator handling (binary system). Instead, LAB with mild reactivity and high flash point (singular system) has been chosen by current generation experiments (Daya Bay,

RENO and SNO+). LAB is the end result of extensive R&D by SNO+, including a search of commercially available scintillators. A similar, improved survey of commercially available liquid scintillators is suggested.

- Large Stokes-shift fluorophores. Most liquid scintillators have long optical transmission in the region of 440-550nm (e.g. LAB has $L_{attn} \sim 30\text{m}$ measured at 450nm emission) where the PMT still has good QE. Identification of fluor/shifter combination optimizing in higher optical emission and light-yield by comparing their fluorescence emission and intrinsic light-yields in different scintillators are the main objectives for this task.
- Temperature effects and time dependent characteristics. Significant improvement in the liquid scintillator light yield could be achieved by lowering the LS temperature (e.g. $\sim 5\%$ more light at 10°C compared to 20°C measured by IHEP). Confirming the temperature dependence and studying time characteristics of LS along with the potential for pulse shape discrimination of different scintillator samples are needed. Pulse shape discrimination may play an important role in intrinsic background rejection in large liquid scintillator detectors. We can finalize the LS temperature and pressure dependence effects utilizing previous experience and upgraded apparatus previously used for Hanohano R&D. Such measurements can be one of the key inputs for detector design and operation.
- Light-yield Measurements. It is well known that quenching affects light output and can lead to reduced scintillation efficiency. The light-yield of surveyed scintillators can be screened by different radioactive sources: α , β , and γ . The selected scintillators' light yield as a function of electron energy can then be studied systematically. The energy response of the liquid scintillator is then to be used for MC simulations.
- This detector is likely to be the largest scintillator detector built in the next 5 years. One potential problem is that laboratory equipment is normally not comparable to the actual size of detector. This creates ambiguity when extrapolating laboratory measurements to the real detector; for instance, both Daya Bay and KamLAND observed $10\sim 15\%$ more scintillation light in the detector than small lab modules. This is likely due to absorption/re-emission or scattering of light propagating through the scintillator. Thus, a satisfactory R&D program needs to build a one-dimensional tube with length close to the detector size to (1) investigate light propagation mechanisms as a function of path-length and (2) verify PE yield at $\sim 30\text{m}$.

4.4 Front-end and trigger electronics

The requirements and specifications of the front-end electronics and trigger system, in particular, the linearity of the charge measurement, dynamic range of time and charge measurements, multiple hit and pileup resolution capability, waveform digitization frequency, types of triggers and their implementation are critical parts of the experiment.

The MBRO LS detector will be a large device with approximately 20,000 PMTs that need to be read out. The readout should address the issue of accurate measurement of low level signals of interest while simultaneously preserving information of large signals originating from muons interacting in the detector. As most of the proposed front end readout will be located inside the detector, reliability of connections and electronics is critical. The development of a readout chain that can be immersed in the detector, digitize and group signals close to the photodetectors and transport the digital information via optical fibers to the DAQ would be desired.

The U.S. team has successfully developed electronic systems meeting such needs in the past. A dynamic range compressor that can preserve the linearity of both low and high amplitude signals is

shown in Ref. [38]. The design will preserve the number of channels and reduce the number of cables that will carry signals out of the detector for further processing. The digitizer for the fifth generation TeV Array with Gsa/s sampling and Experimental Trigger (TARGET) [39] can be used in MBRO experiments. It is an ASIC that contains 16 channels of transient waveform recorder that was designed to be used in highly pixelated photon detectors for large neutrino and muon detectors.

The details of how to design and deploy a reliable system is central to such R&D efforts. In the past, the U.S. team has developed electronics deployed in other experiments with little to no access and we are quite confident that a solution to achieve the necessary reliability is possible.

4.5 Detector energy response calibration

As one of the most crucial requirements, detector energy response calibration should be one of the U.S. R&D program's main prioritized focuses. We have considered various options in calibrating the detector using a combined approach based on our experiences obtained in LS detector experiments like KamLAND and Daya Bay [34, 40, 41]. Due to the size of the MBRO detectors, uniformity plays a more significant role than smaller detectors which have been constructed in the past. We are considering options of dissolving short-lived radioactive isotopes to calibrate the detector response besides the mature approaches using the uniformly distribution intrinsic events like spallation neutrons. To have precise position dependence studies, we are studying multiple ways of deploy point calibration sources to the whole volume. We know that different types of particles exhibit different energy responses in a LS detector, thus it is critical to select the most suitable calibration sources to reduce the non-linearity uncertainties. We are also studying different types of radioactive sources.

We learned from Daya Bay and KamLAND experiments that multiple energy scale models can generally be constructed with different types calibration samples and different emphases. The various models on one hand explore different aspects of the detector, which is good for us to fully understand our detector. On the other hand, at the same time, it unavoidably increases the energy scale uncertainties and functional form complexities which decrease the sensitivity of the experiment to MH as shown in Sec.2.2. The complementarities or conflicts depending on our points of view, among various models are largely due to the lack of positron calibration sources and the lack of continuous coverage over the entire IBD spectrum. In view of this, we are considering to build a positron accelerator on-site which would provide mono-energetic positrons to calibrate the detector for IBD events. After reviewing different technologies, we think positron pelletron is reliable and would be able to deliver mono-energetic positrons that cover the IBD spectrum continuously. Its dimension is on the order of $\sim 10\text{m}$ thus can fit in JUNO or RENO-50 type experimental halls easily. Based on survey of existing facilities, 0.5 to 6.5 MeV positron beams can be produced with an accuracy of $\Delta E/E \leq 10^{-4}$ [42]. The pelletron can also switch to use electron sources thus provide electron beams in the same energy range.

With both the calibration source and the tunable positron/electron pelletron approaches, we believe a highly accurate energy response model of MBRO LS detectors can be obtained to meet the needs of MH sensitivity and precision measurements. Naturally, the following R&Ds are needed in order to mount a successful calibration system for MBRO experiments:

- Develop a liquid scintillator test chamber for the precise laboratory study of the light response and non-linearity of the liquid scintillator with the capability to characterize in-situ calibration sources. This will provide a precise characterization of calibration sources in the LS and allow tests of secondary effects from shielding and source encapsulation.
- Develop concepts for the deployment and precise positioning of radioactive and light sources throughout a 30m large detector.

- Develop a concept for the injecting and distributing of uniformly distributed short-lived radioactive isotopes for calibration of the detector volume.
- Develop a tunable positron/electron gun in the energy range of 1-8 MeV for continuous calibration over the reactor antineutrino spectrum. Pelletron technology is an attractive option for this purpose.

5 Other potential physics topics

With 10-20 kt LS detectors underground, MBRO experiments offer many other physics opportunities. We only list a few highlights below:

- **Supernova Neutrinos:**
It is estimated that for a typical (3×10^{53} erg) supernova 10 kpc away, ~ 3000 inverse beta decay events can be detected, together with ~ 3000 events in other visible channels.
- **Geoneutrinos:**
With a 20 kt LS detector, JUNO expects to observe ~ 750 geoneutrino events per year. The reactor background in the energy range of geoneutrinos (1.8 – 3.3 MeV) is about 4 times larger. The difference in shape and time dependence will help to extract the geoneutrino signals.
- **Proton Decay:**
If nanosecond timing resolution can be reached, MBRO LS detectors will be in good position to measure proton decay in the decay channel $p \rightarrow K^+ \bar{\nu}$. Scaling from LENA's estimation [43], a lower limit of proton lifetime, concerning the decay channel investigated, of $\tau > 2.4 \times 10^{34}$ y (at 90% C.L.) could be reached in 10 years by JUNO.

6 Summary and conclusions

Medium-baseline reactor neutrino experiments using massive LS detectors provide a unique opportunity to determine the neutrino mass hierarchy. Such experiments have unprecedented detector performance requirements which have not been realized before. Our independent calculation confirms the sensitivities claimed by other groups in the form of $\Delta\chi^2$ values under near ideal condition with different assumptions on the LS detector performance. In addition to the widely recognized and accepted no-go condition of energy resolution worse than $\sim 3\%/\sqrt{E(\text{MeV})}$, we find that understanding the uncertainty of MBRO LS detectors' energy non-linearity plays a crucial role in its sensitivity to MH. Under certain types of non-linear bias, sensitivity will be significantly reduced. A dedicated energy scale calibration system must be developed to control the energy scale uncertainty.

We find that a good knowledge of the reactor spectrum can relax the requirements on the energy calibration as the spectrum is correlated between different energies. If understandings on reactor spectrum won't be improved significantly during the course of MBRO experiments, Fourier method or the spectrum ratio method are less sensitive to the reactor spectrum but the requirement in the absolute energy scale becomes more stringent. Under such scenarios, we recognize that a second detector at a suitable baseline $\sim 30\text{km}$ can mitigate the stringent requirement on energy scale thus improve the sensitivity.

Besides experimental challenges, we also find due to the discrete nature of MH, the $\sqrt{\Delta\chi^2}$ rule of setting measurement confidence levels does not apply in MH determination. Combining all factors, we find the best scenario of current MBRO experiment proposals is to reach $2 \sim 2.5\sigma$ sensitivity in MH ($\Delta\chi^2 = 16 \sim 25$).

MBRO experiments offer rich physics programs which extend from precision neutrino oscillation parameter measurements, planetary science to the observation of geoneutrinos, test of grand unification theories via proton decay studies and, potentially, study astrophysics via ex-territorial neutrinos. The oscillation parameters' precise measurements are guaranteed to reach sub-percent level should we reach the designed performance of MBRO detectors. Such precision results would enable a future direct unitarity test of the neutrino mixing PMNS matrix's to $\sim 1\%$ level. Recent studies show that combining the data from MBRO experiments with next generation long-baseline beam neutrino and atmospheric neutrino experiments like NO ν A, T2K, INO, PINGU, and ORCA can enhance the sensitivity to MH. The power lies in that the atmospheric mass-squared splitting is constrained systematically different in MBRO experiments and in beam/atmospheric neutrino experiments. The forthcoming neutrinoless double beta decay experiments will also benefit from precise measurements of the solar mixing angle as it helps to improve the constraints on absolute neutrino mass $\langle m_{\beta\beta} \rangle$. In order to reach the desired accuracy in the MBRO LS detectors' energy responses, we have considered various calibration strategies. By combining radioactive sources deployed in multiple ways and a positron pelletron with tunable mono-energetic positron beams, we can calibrate the detector with complete coverage in both spatial aspect and energy spectrum aspect.

MBRO experiments face many unprecedented challenges while offering great physics opportunities. Well-designed R&D programs are needed to ensure its success. The U.S. team is experienced in many respects of such experiments thus is in a very good position to initiate a US R&D program for MBRO experiments. The current estimated cost of JUNO in China is a few hundred million dollars with an estimated 5 years for construction. Primary support for this experiment from Chinese funding agencies looks very promising and there are substantial opportunities for international collaboration. R&D and site investigations in China are underway. Data taking could begin around 2020. A similar proposal named RENO-50 has been proposed in South Korea with slightly shorter baseline and 90% of the JUNO's target mass. A U.S. R&D program will ensure the U.S. team master the key technologies of the critical experimental components of MBRO experiments and make irreplaceable contributions in the forthcoming MH discovery and precision neutrino physics era.

References

- [1] **Daya Bay** Collaboration, F. An *et. al.*, *Observation of electron-antineutrino disappearance at Daya Bay*, *Phys.Rev.Lett.* **108** (2012) 171803, [[arXiv:1203.1669](#)].
- [2] **Daya Bay** Collaboration, F. An *et. al.*, *Improved Measurement of Electron Antineutrino Disappearance at Daya Bay*, *Chin. Phys.* **C37** (2013) 011001, [[arXiv:1210.6327](#)].
- [3] **RENO** Collaboration, J. Ahn *et. al.*, *Observation of Reactor Electron Antineutrino Disappearance in the RENO Experiment*, *Phys.Rev.Lett.* **108** (2012) 191802, [[arXiv:1204.0626](#)].
- [4] S. Petcov and M. Piai, *The LMA MSW solution of the solar neutrino problem, inverted neutrino mass hierarchy and reactor neutrino experiments*, *Phys.Lett.* **B533** (2002) 94–106, [[hep-ph/0112074](#)].
- [5] S. Choubey, S. Petcov, and M. Piai, *Precision neutrino oscillation physics with an intermediate baseline reactor neutrino experiment*, *Phys.Rev.* **D68** (2003) 113006, [[hep-ph/0306017](#)].
- [6] A. de Gouvea, J. Jenkins, and B. Kayser, *Neutrino mass hierarchy, vacuum oscillations, and vanishing $|U_{e3}|$* , *Phys.Rev.* **D71** (2005) 113009, [[hep-ph/0503079](#)].

- [7] J. Learned, S. T. Dye, S. Pakvasa, and R. C. Svoboda, *Determination of neutrino mass hierarchy and θ_{13} with a remote detector of reactor antineutrinos*, *Phys.Rev.* **D78** (2008) 071302, [[hep-ex/0612022](#)].
- [8] H. Minakata, H. Nunokawa, S. J. Parke, and R. Zukanovich Funchal, *Determination of the neutrino mass hierarchy via the phase of the disappearance oscillation probability with a monochromatic anti-electron-neutrino source*, *Phys.Rev.* **D76** (2007) 053004, [[hep-ph/0701151](#)].
- [9] S. J. Parke, H. Minakata, H. Nunokawa, and R. Z. Funchal, *Mass Hierarchy via Mossbauer and Reactor Neutrinos*, *Nucl.Phys.Proc.Suppl.* **188** (2009) 115–117, [[arXiv:0812.1879](#)].
- [10] L. Zhan, Y. Wang, J. Cao, and L. Wen, *Determination of the Neutrino Mass Hierarchy at an Intermediate Baseline*, *Phys.Rev.* **D78** (2008) 111103, [[arXiv:0807.3203](#)].
- [11] L. Zhan, Y. Wang, J. Cao, and L. Wen, *Experimental Requirements to Determine the Neutrino Mass Hierarchy Using Reactor Neutrinos*, *Phys.Rev.* **D79** (2009) 073007, [[arXiv:0901.2976](#)].
- [12] E. Ciuffoli, J. Evslin, and X. Zhang, *The Neutrino Mass Hierarchy at Reactor Experiments now that θ_{13} is Large*, *JHEP* **1303** (2013) 016, [[arXiv:1208.1991](#)].
- [13] S.-F. Ge, K. Hagiwara, N. Okamura, and Y. Takaesu, *Determination of mass hierarchy with medium baseline reactor neutrino experiments*, *JHEP* **1305** (2013) 131, [[arXiv:1210.8141](#)].
- [14] F. Capozzi, E. Lisi, and A. Marrone, *Neutrino mass hierarchy and electron neutrino oscillation parameters with one hundred thousand reactor events*, [arXiv:1309.1638](#).
- [15] **LBNE** Collaboration, T. Akiri *et. al.*, *The 2010 Interim Report of the Long-Baseline Neutrino Experiment Collaboration Physics Working Groups*, [arXiv:1110.6249](#).
- [16] S. Bertolucci, A. Blondel, A. Cervera, A. Donini, M. Dracos, *et. al.*, *European Strategy for Accelerator-Based Neutrino Physics*, [arXiv:1208.0512](#).
- [17] M. Diwan, R. Edgecock, T. Hasegawa, T. Patzak, M. Shiozawa, *et. al.*, *Future long-baseline neutrino facilities and detectors*, *Adv.High Energy Phys.* **2013** (2013) 460123.
- [18] Y.-F. Li, J. Cao, Y. Wang, and L. Zhan, *Unambiguous Determination of the Neutrino Mass Hierarchy Using Reactor Neutrinos*, [arXiv:1303.6733](#).
- [19] W. Rodejohann, *Neutrinoless double beta decay and neutrino physics*, *J.Phys.* **G39** (2012) 124008, [[arXiv:1206.2560](#)].
- [20] **RENO-50** Collaboration, R. collaboration, *RENO-50*, in *International Workshop on RENO-50 toward Neutrino Mass Hierarchy*, 2013.
- [21] X. Qian, D. Dwyer, R. McKeown, P. Vogel, W. Wang, *et. al.*, *Mass Hierarchy Resolution in Reactor Anti-neutrino Experiments: Parameter Degeneracies and Detector Energy Response*, *PRD*, **87**, **033005** (2013) [[arXiv:1208.1551](#)].
- [22] X. Qian, A. Tan, W. Wang, J. Ling, R. McKeown, *et. al.*, *Statistical Evaluation of Experimental Determinations of Neutrino Mass Hierarchy*, *Phys.Rev.* **D86** (2012) 113011, [[arXiv:1210.3651](#)].
- [23] **KamLAND** Collaboration, S. Abe *et. al.*, *Precision measurement of neutrino oscillation parameters with kamland*, *Phys. Rev. Lett.* **100** (Jun, 2008) 221803.

- [24] **Daya Bay** Collaboration, Daya Bay, “to be published.” 2013.
- [25] P. Huber, *On the determination of anti-neutrino spectra from nuclear reactors*, *Phys.Rev.* **C84** (2011) 024617, [arXiv:1106.0687].
- [26] T. Mueller, D. Lhuillier, M. Fallot, A. Letourneau, S. Cormon, *et. al.*, *Improved Predictions of Reactor Antineutrino Spectra*, *Phys.Rev.* **C83** (2011) 054615, [arXiv:1101.2663].
- [27] E. Ciuffoli, J. Evslin, Z. Wang, C. Yang, X. Zhang, *et. al.*, *Medium Baseline Reactor Neutrino Experiments with 2 Identical Detectors*, arXiv:1211.6818.
- [28] X. Qian, C. Zhang, M. Diwan, and P. Vogel, *Unitarity Tests of the Neutrino Mixing Matrix*, arXiv:1308.5700.
- [29] **IceCube** Collaboration, IceCube Collaboration, *PINGU Sensitivity to the Neutrino Mass Hierarchy*, arXiv:1306.5846.
- [30] M. Ribordy and A. Y. Smirnov, *Improving the neutrino mass hierarchy identification with inelasticity measurement in PINGU and ORCA*, arXiv:1303.0758.
- [31] M. Blennow and T. Schwetz, *Determination of the neutrino mass ordering by combining PINGU and Daya Bay II*, arXiv:1306.3988.
- [32] Y. Wang, *Daya Bay II: current status and future plan*, in *Daya Bay II First Meeting*, 2013.
- [33] Y. Wang, *Daya Bay II: the next generation reactor neutrino experiment*, in *NuFACT 2012*, 2012.
- [34] B. E. Berger *et. al.*, *The KamLAND full-volume calibration system*, *Journal of Instrumentation* **4** (Apr., 2009) 4017, [arXiv:0903.0441].
- [35] M. Diwan, J. Dolph, J. Ling, T. Russo, R. Sharma, *et. al.*, *Underwater implosions of large format photo-multiplier tubes*, *Nucl.Instrum.Meth.* **A670** (2012) 61–67.
- [36] M. Diwan, J. Dolph, J. Ling, T. Russo, R. Sharma, *et. al.*, *Implosion chain reaction mitigation in underwater assemblies of photomultiplier tubes*, accepted by *NIMA* (2013).
- [37] P. DeVore, D. Escontrias, T. Koblesky, C. Lin, D. Liu, *et. al.*, *Light-weight Flexible Magnetic Shields For Large-Aperture Photomultiplier Tubes*, arXiv:1309.5415.
- [38] W. Cleland *et. al.*, *Dynamic range compression in liquid argon calorimeter*, *BNL 63670* (1996).
- [39] K. Bechtol, S. Funk, A. Okumura, L. Ruckman, A. Simons, *et. al.*, *TARGET: A multi-channel digitizer chip for very-high-energy gamma-ray telescopes*, *Astropart.Phys.* **36** (2012) 156–165, [arXiv:1105.1832].
- [40] J. Liu *et. al.*, *Automated Calibration System for a High-Precision Measurement of Neutrino Mixing Angle θ_{13} with the Daya Bay Antineutrino Detectors*, *ArXiv e-prints* (May, 2013) [arXiv:1305.2248].
- [41] H. Huang *et. al.*, *Manual Calibration System for Daya Bay Reactor Neutrino Experiment*, *ArXiv e-prints* (May, 2013) [arXiv:1305.2343].
- [42] W. Bauer, *The Stuttgart Positron Beam, its Performance and Recent Experiments*, *Nucl.Instrum.Meth.* **B50** (1990) 300.
- [43] **LENA** Collaboration, M. Wurm *et. al.*, *The next-generation liquid-scintillator neutrino observatory LENA*, *Astropart.Phys.* **35** (2012) 685–732, [arXiv:1104.5620].